ELSEVIER

1 December 1995

Optics Communications 121 (1995) 95–102

OPTICS COMMUNICATIONS

Advanced phase knife technique

A.V. Larichev [a], I.P. Nikolaev [a], S. Costamagna [b], P. Violino [b]

[a] *International Laser Center, Moscow State University, 119899 Moscow, Russia*

[b] *Department of Experimental Physics, University of Turin, Via P. Giuria 1, 10125 Torino, Italy*

Received 22 March 1995; revised version received 13 June 1995

Abstract

Small-scale phase inhomogeneities visualization methods based on phase knife filtering are considered. A new modification of such a technique with controllable lower threshold frequency is suggested: when transversally displaced from the center of the Fourier plane, the phase knife demonstrated some new features. Phase-to-intensity transfer function of the filtering system for arbitrary depth of harmonical phase modulation is obtained analytically, numerically and experimentally. Possibility of optical implementation of "exclusive or" (XOR) logical operation by means of 2D phase knife is shown.

1. Introduction

The problem of phase retrieval of a light wave passed through an optically inhomogeneous medium as well as the problem of diagnostics of phase distortions have been the subject of extensive studies. Several a posteriori algorithms based on the analysis of the intensity distribution of transformed input field (for example, power spectrum i.e. the Fourier transform) were suggested to solve these problems [1,2]. Another way is to use a wavefront sensor (like a Shack Hartmann one) typical to adaptive optics systems [3]. Usually systems of this kind are able to operate only with phase distortions whose spatial scale is not less than $a/10$, where a is the working aperture. Recent achievements in applications of nonlinear optical systems with spatially distributed feedback are evidence of the possibility of a high resolution (up to $a/1000$) wavefront correction [4,5]. However, it is very important to find out an optimal technique to generate a pattern of controlling intensity (feedback error signal). Complex spatial filtration techniques seem to be very promising for this purpose, although their advantages become visible only when dealing with small-scale phase inhomogeneities.

Fundamental experiments of Zernike and Focault prompted wide investigations with two spatial filters named after them [6]. At the same time the method of phase visualization by phase knife is much less developed [7]. Only a few particular cases have been examined, and their mathematical description is valid only for phase modulation of small amplitude (much less than unity). However, it was found that this method and its modifications had some features suggesting promising applications to the above-mentioned tasks. Furthermore, the development of photo-lithographic technique ensured a possibility to produce phase filters of this type having sufficient quality. Using a modern liquid crystal light valve (LCLV) [8] one becomes able to generate a phase object of desired transversal distribution and with a modulation depth of almost 2π, that significantly simplifies the experimental investigation of the filters.

In this paper we present theoretical and experimental methods for studying the filtering system phase-to-amplitude transfer function, i.e. the law of transformation of sinusoidal phase modulation into an

SSDI 0030-4018(95)00446-7

amplitude one. Knowing this law, one can develop a mathematical model of the optical feedback system with the investigated spatial filter being a controlling intensity generator.

2. Optical scheme

A spatial filtration of patterns is among the well-known methods of image processing. We consider here a transformation of pure phase objects by means of the optical scheme shown in Fig. 1a. The image recorded on a film slide SI is illuminated by collimated light and is projected on the photoconductor surface of the LCLV. Ls is an incoherent light source, and Cd is an optical condenser. According to the intensity distribution in the projected slide, the LCLV modulates the transversal phase distribution of laser beam Lb being reflected by its second (liquid crystal) surface. The beam is previously expanded by means of a telescopic system. The spatial filter Sf is placed in the Fourier-plane of "4-F" imaging system whose object plane is a liquid crystal slice of LCLV, i.e. a phase representation of the slide SI. The filtered image is collected on the screen Sc and digitized by means of an S-video camera with a frame grabber in order to carry out subsequent computations. This optical scheme may be also considered as a phase-to-amplitude field transformer being a part of a nonlinear optical system with spatially distributed feedback [9].

We investigated the phase knife produced as a glass plate with a step-like thickness modulation. It is shown in Fig. 1b (sketch) and Fig. 1c (photo of the phase knife we used, made by phase-contrast microscopy). The filter consists of four quadrants, two of them (II and IV) introducing an additional phase shift $\pm\pi$ into

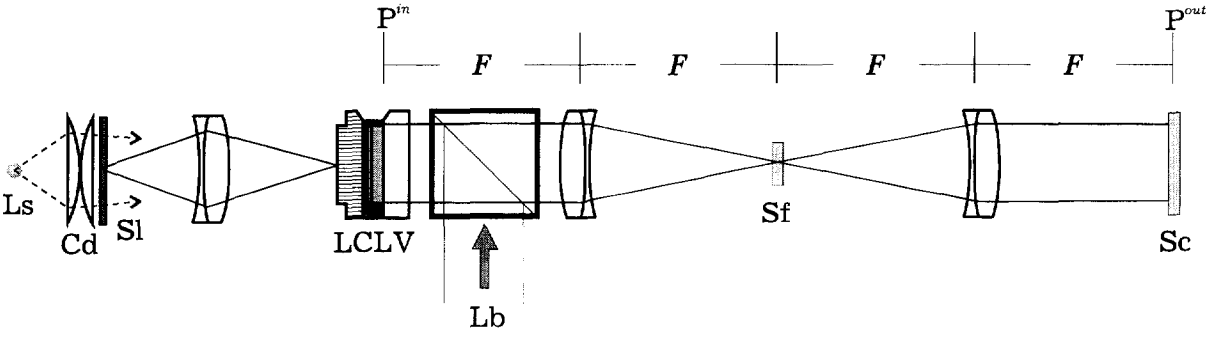

a

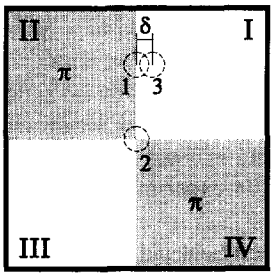

b

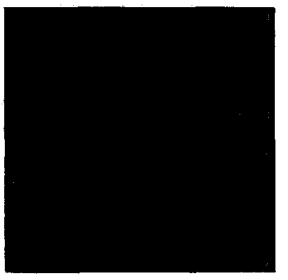

c

Fig. 1. Experimental setup: (a) optical scheme, (b) sketch of the spatial filter; dashed circles correspond to the Airy disc location in the case of: 1 – 1D centered, 2 – 2D centered and 3 – displaced operating regimes, (c) phase-contrast microscope picture of the spatial filter.

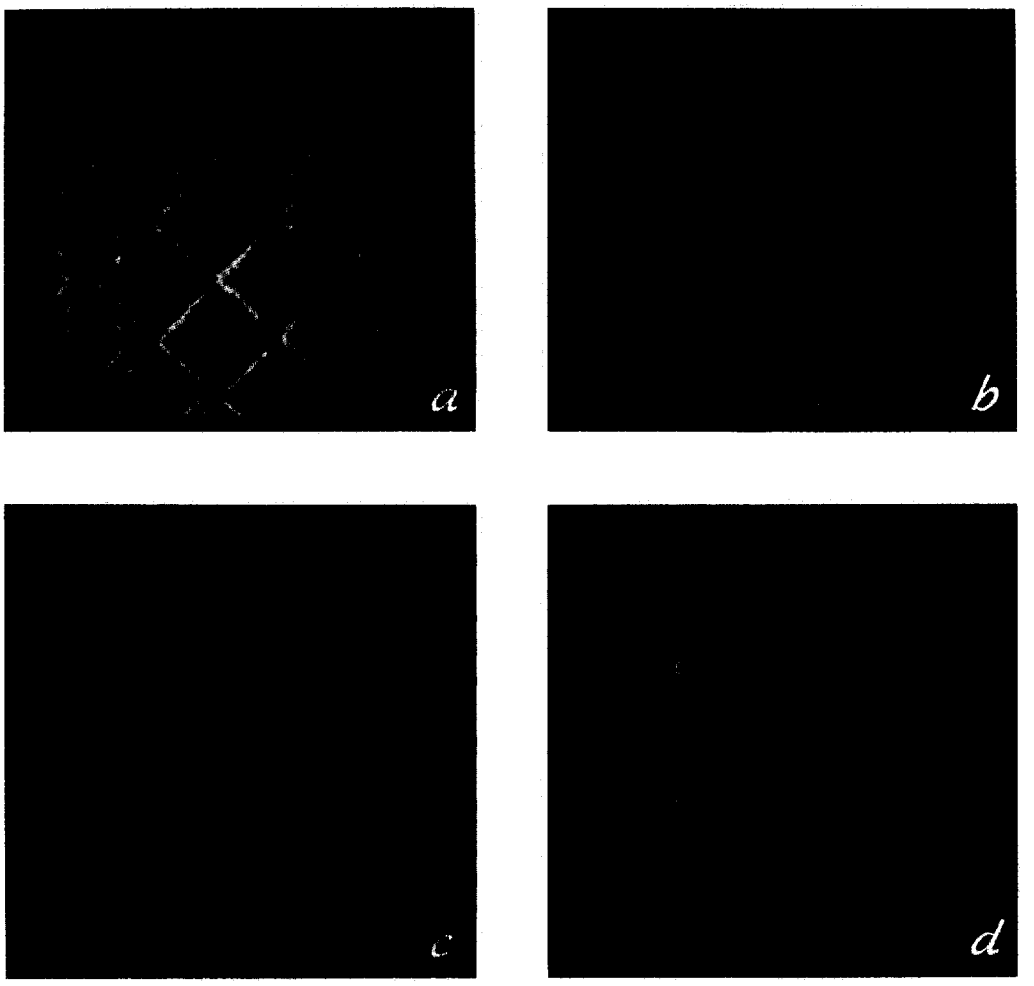

Fig. 2. Visualization of 2D rectangular phase grating by the centered 1D phase knife with vertical edge: (a, b) experimental photographs, (c, d) numerical simulation.

the radiation passing through them. The step thickness is adjusted to the wavelength of 0.514 μm, our source being an Ar^+ laser. The filter can be used in several regimes, differing by the location of zero-order of the input field spectrum respectively to its edges.

To begin with, we consider the simplest case – 1D phase knife with only one "working" border between two quadrants. The corresponding location of Airy disc within the filter surface is labeled as 1 in Fig. 1b. In order to illustrate how the system works we choose as a phase object the rectangular 2D grating of amplitude π (shown in Fig. 5a). Figs. 2a and 2c represent experimental photo's and results of numerical simulation of intensity distribution within the screen Sc. The filter edge is oriented vertically. The filtering system visualizes a gradient region of the phase distribution, as it is stated in [7]. However, if one of the orthogonal sub-gratings is oriented parallel to the filter edge, its power spectrum, widened by aperture influence, is divided in half by the edge. It leads thus to suppression of this sub-grating after the filtration. Then the output intensity pattern becomes a great deal different (Figs. 2b and 2d). To prevent this effect the following condition must be satisfied:

$$\alpha > 1/n\,, \tag{1}$$

where α is the angle between a significant spectral component κ of input image and filter edge direction,

and n is the corresponding magnitude $|\boldsymbol{\kappa}|$, measured in periods per aperture. This condition applies for each $\boldsymbol{\kappa}$ and follows just from geometry of the power spectrum within the Fourier plane. So every spectral component satisfying (1) is treated by the filter the same way. It allows to use 1D approach for all these harmonics in spite of the variety of their orientation in space.

3. The Hilbert transform carried out by phase knife

To avoid indefiniteness connected with essential anisotropy of the filter we examined in detail a quasi-1D case, when the field complex amplitude was only a function of transversal coordinate x. Suppose the knife edge is oriented orthogonally to x axis, in that case the filter performs the 1D Hilbert transform:

$$A_{\text{out}}(x) = \hat{H}_x[A_{\text{in}}(x)] = A_{\text{in}}(x) \otimes \text{PV}\,\frac{1}{\pi x}$$

$$= \frac{1}{\pi}\,\text{PV}\int_{-\infty}^{\infty} \frac{A_{\text{in}}(\xi)}{\xi - x}\,\mathrm{d}\xi, \qquad (2)$$

where $A_{\text{in}}(x)$ and $A_{\text{out}}(x)$ are the complex amplitudes of the light field within plane P^{in} (input) and P^{out} (output) according to Fig. 1a; PV indicates the principal value of the convolution integral.

Let us calculate the transfer function of the visualizing system, i.e. κ'-spectral component amplitude of output intensity $I^{\kappa'}_{\text{out}}$ as a function of an amplitude c_0 of harmonical phase modulation of input field:

$$A_{\text{in}}(x) = \exp(\mathrm{i}\varphi_{\text{in}}(x)]$$

$$= \exp[\mathrm{i}c_0\cos(\kappa_0 x)]\,, \qquad (3)$$

input intensity is uniform and equal to unity. $I^{\kappa'}_{\text{out}}$ stays for the leading term in the Fourier series representation of $I_{\text{out}}(x)$, i.e. it is not necessarily $\kappa' = \kappa_0$.

Usually for the calculation of the intensity distribution within the filter output plane the scalar diffraction theory is applied [10]. This analytical technique is useful for controlling the large-scale phase fluctuations. However, if the spatial period of the input phase grating is less than $a/1.22$ (meaning that the diffraction spot of the corresponding spectral component is not crossed by the filter edge), then the Neumann series approach becomes preferable.

In that case the procedure of analytical transfer function determination for the Fourier-optics systems is the following [11]: the function $A_{\text{in}}(x)$ must be represented in the Neumann series form, and then every complex amplitude of its spectrum is multiplied by the value of the complex transmission function of the spatial filter corresponding to its frequency κ_0. Taking into account, for example, the first four terms of the Neumann expansion one can get for output intensity:

$$I_{\text{out}}(x) = \hat{I}_{\text{out}} - I^{2\kappa_0}_{\text{out}}\cos(2\kappa_0 x) + \ldots\,, \qquad (4)$$

where uniform intensity and amplitude of doubled frequency intensity modulation are:

$$\hat{I}_{\text{out}} = 2\{J_1^2(c_0) + J_2^2(c_0) + J_3^2(c_0) + \ldots\}\,,$$

$$I^{2\kappa_0}_{\text{out}} = 2\{J_1^2(c_0) + 2J_1(c_0)J_3(c_0) + \ldots\}\,, \qquad (5)$$

where J_n is the Bessel function of order n. Expressions (4), (5) have a 95% accuracy for $c_0 \leqslant 2$, and if $c_0 \ll 1$ we obtain a well-known [7] formula:

$$I_{\text{out}}(x) \approx \frac{c_0^2}{2}\,(1 - \cos(2\kappa_0 x))\,. \qquad (6)$$

More precise expression for transfer function (5) in case of strong phase modulation may be derived by taking into account more terms in the Neumann representation of (3). In any case the output intensity spatial spectrum does not include κ_0-frequency component and its components are all multiples of $2\kappa_0$.

With the aim of measuring the transfer function experimentally we made a special slide with 1D sinusoidal modulation of opacity. This slide ensured a sinusoidal controlling light distribution for LCLV, and phase modulation amplitude was varied according to the intensity of the incoherent light source Ls. To calculate the corresponding depth of phase modulation arising in the liquid crystal slice (plane P^{in} in Fig. 1a) we measured the sensitivity curve of LCLV by near-field diffraction technique (phase visualization by defocus) [6,12]. Such a method ensures the accuracy of modulation amplitude experimental measurement of about 0.05 rad. This value is mostly caused by LCLV internal inhomogeneity and air blowing, that can not be accounted adequately.

The working aperture was 1 cm and the investigated sinusoidal grating had 10 periods per aperture. In order

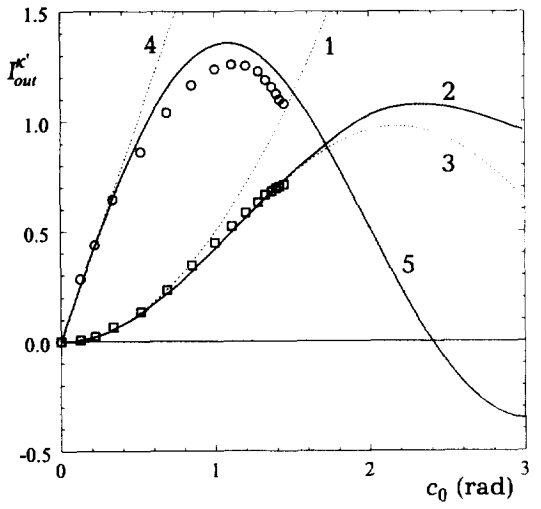

Fig. 3. Transfer function plots. For centered phase knife ($\kappa' = 2\kappa_0$): 1 – parabolic approximation (Eq. (6)); 2 – numerical simulation; 3 – Bessel approximation (Eq. (5)); also experimental data (circle dots). For displaced phase knife ($\kappa' = \kappa_0$): 4 – linear approximation (Eq. (10)); 5 – exact expression (Eq. (9)); also experimental data (square dots).

to prevent some boundary effects influence we measured the spectrum of output intensity only within a central part of the beam (3–4 periods). The Hilbert transform is very sensitive to every small tilt of the beam caused by vibration or air blowing [13]. So we used time-averaging to reduce these effects. Fig. 3 represents three transfer function curves (labeled as 1–3 respectively): approximate (Eq. (6)), "exact" (numerically calculated) and approximate (Eq. (5)) plots of $I_{out}^{2\kappa_0}$ as a function of c_0, compared with experimental data (circle dots). With the LCLV we used we can get the maximal nonlinear phase shift of about 2π. But for a transfer function measurements only a linear part of LCLV sensitivity curve should be used. So we limited the value of experimentally achieved phase modulation to 1.5 rad which corresponded to a full modulation depth around π.

4. Transversally displaced phase knife

While operating with the experimental set-up we found out that the output pattern is critically dependent on accuracy of alignment of the filter edge at the center of the Fourier-plane. Usually this feature is considered as an interfering factor making optical implementation of the Hilbert transform more complicated in mechanical requirements. We investigated separately the case of phase knife transversal displacement and looked for essential properties of such a transform.

Suppose the spatial filter placed at such a position within the Fourier-plane that δ is a distance between its edge and zero frequency spot center (area 3 in Fig. 1b). It means that the edge position in spectral area is $\eta = k\delta/F$, where k is the laser radiation wavenumber and F is the lens focal distance. Such a phase knife is no longer producing the Hilbert transform, and instead of (2) one can obtain

$$A_{out}(x) = A_{in}(x) \otimes \mathrm{PV}\,\frac{\exp(i\eta x)}{\pi x}$$

$$= e^{-i\eta x}\hat{H}_x[A_{in}(x)e^{i\eta x}] \,. \qquad (7)$$

Thus, the Hilbert transform may be considered as a particular case (when $\eta = 0$) of transform (7). We chose the filter displacement δ in such a way that the Airy disc lied wholly within quadrant I of the phase-shifting plate. Then the zero component is no longer suppressed by the filter edge and interferes with the other spectral components. The Neumann series approach allows us to obtain the transfer function for $\kappa_0 > |\eta|$:

$$I_{out}(x) = \hat{I}_{out} + I_{out}^{\kappa_0}\sin(\kappa_0 x) + \ldots \,, \qquad (8)$$

where uniform intensity and amplitude of intensity modulation are

$$\hat{I}_{out} = J_0^2(c_0) + 2\{J_1^2(c_0) + J_2^2(c_0) + J_3^2(c_0) + \ldots\} \,,$$

$$I_{out}^{\kappa_0} = 4\,\mathrm{sgn}(\eta) J_0(c_0) J_1(c_0) \,. \qquad (9)$$

Note that the last expression is an exact one and its approximation for $c_0 \ll 1$ is the following:

$$I_{out}^{\kappa_0} \approx \pm 2c_0 \,. \qquad (10)$$

The essential difference between (8), (9) and (4), (5) is the presence of output intensity modulation at the same frequency as in the input phase, and there is a quarter-period shift between functions $\varphi_{in}(x)$ and $I_{out}(x)$. Photographs of the beam central part presented in Fig. 4 illustrate this difference between a "classical" phase knife (b) and a displaced one (c).

Since for $\kappa_0 < |\eta|$ there is no phase shift between "$+\kappa_0$" and "$-\kappa_0$" Fourier spectrum components then no visualization of phase modulation with spatial

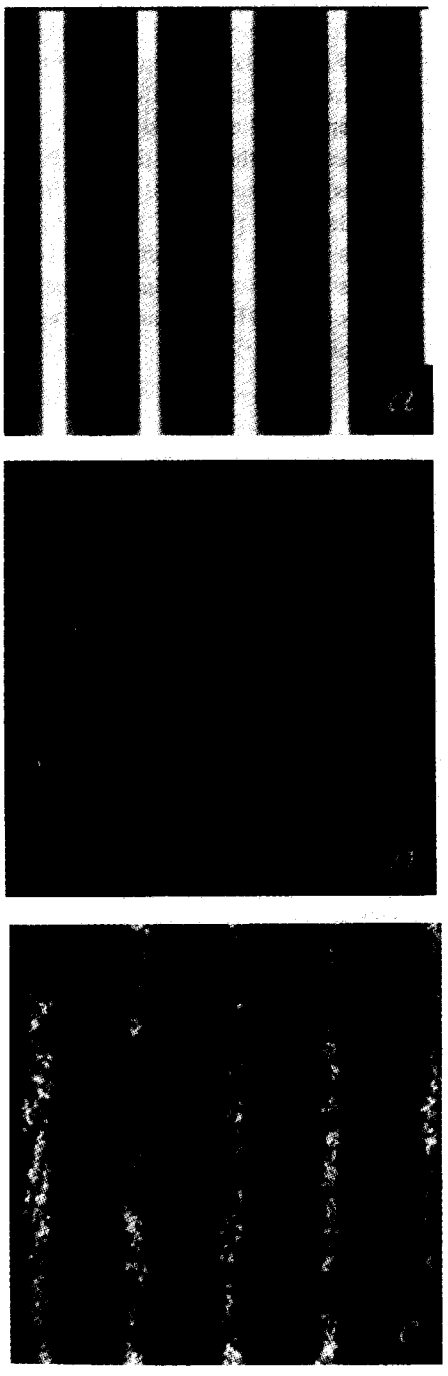

Fig. 4. The experimental photographs of 1D sinusoidal phase grating processing: (a) input slide, (b) transform by centered phase knife (the Hilbert transform), (c) transform by displaced phase knife.

frequency $\kappa_0 < |\eta|$ can be observed. Thus, by moving the phase knife across the Fourier plane one can choose the threshold visualization frequency limiting the sensitivity of the system to low order aberrations.

Experimental data of the transfer function measurements in comparison with theoretical plots are shown in Fig. 3 (plots 4, 5 and square dots). A monotonous dependence is observed only for phase modulation amplitude $c_0 < 1.1$; for $c_0 > 2.4$ the inversion of contrast takes place. A good accordance between theoretical results and experimental data exists, showing the potential use of such an experimental technique for quantitative measurements. On the other hand, it means that the investigated phase knife may be adequately accounted in the mathematical model of the feedback system, which requires a knowledge of the transfer function of feedback loop [9].

5. An optical implementation of logical XOR operation

A general investigation of 2D phase knife (area 2 in Fig. 1b) seems to be rather difficult due to its anisotropy. An analysis of an output pattern is especially complicated in the case when some spectral components of the phase object are located at the filter edge. Also it is difficult, owing to technological problems, to obtain a real phase knife (Fig. 1c) fitting precisely an "ideal" one in its central part.

However, if one satisfies the condition (1) an interesting effect is observed, when operating with a phase object (Fig. 5a) with a cross-like spatial spectrum (Fig. 5b). The orthogonal components appear in a different regions of the filter and consequently after passing through it become anti-phase. This is responsible for some features of the output intensity pattern, presented in Fig. 5: (c) numeric computation, (d) experimental photo. The regions corresponding to bright lines crossings in Fig. 5a are dark in the output intensity pattern. Thus, 2D phase knife may be considered as a device producing an optical implementation of "exclusive or" logical operation between two barcode-like orthogonal patterns.

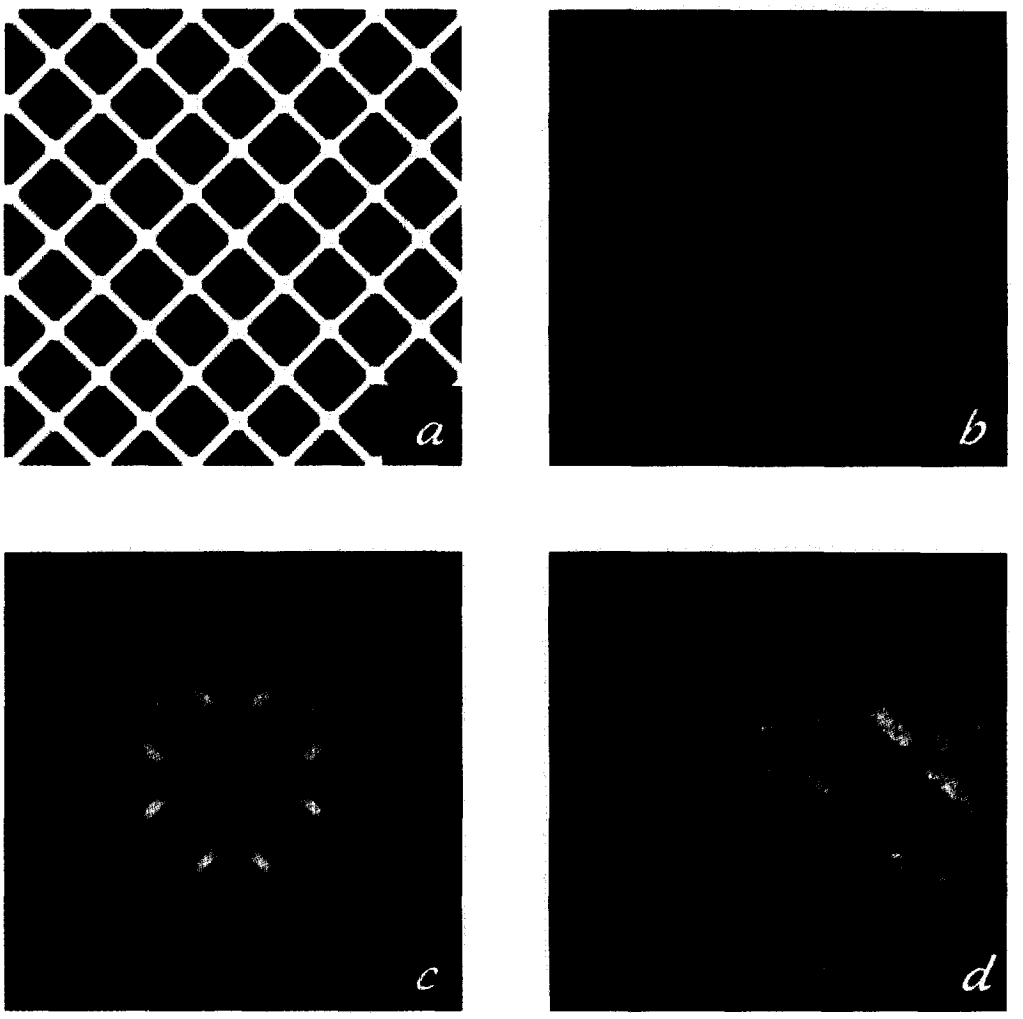

Fig. 5. "Exclusive or" operation by means of 2D centered phase knife: (a) input phase object, (b) its power spectrum, (c, d) output intensity patterns: numerical simulation and experiment, respectively.

6. Conclusions

We suggested and investigated theoretically and experimentally the operating regime of 1D phase knife when it is transversally displaced from the center of the Fourier-plane. The main observed features of image-filtering optical system involving such a device are the following:

(i) high sensitivity and high contrast of phase visualization;

(ii) appearance of the first harmonic shifted by quarter-period in output intensity spectrum;

(iii) controllable edge frequency for phase visualization;

(iv) little sensitivity to tilts of the beam and vibrations.

All above-mentioned features indicate that displaced phase knife seems to be useful as an element of nonlinear optical system with spatially distributed feedback. It may also be used for "pure" image processing applications: a technique for implementation of logical XOR between two binary-type orthogonal patterns is suggested.

Acknowledgements

We wish to thank A. Karpov for help in programming of 2D numeric computations and V. Wataghin for fruitful discussions. This work has been carried out under a special agreement between Moscow State University and the University of Torino. The experimental part was funded by the Italian National Research Council and the Italian Ministry for University and Scientific Research.

References

[1] R.W. Gerchberg and W.O. Saxton, Optik 35 (1972) 237.
[2] N. Nakajima and B. Saleh, Appl. Optics 33 (1994) 821.
[3] J.W. Hardy, Proc. IEEE 66 (1976) 651.
[4] M.A. Vorontsov, V.A. Katulin and A.F. Naumov, Optics Comm. 71 (1989) 35.
[5] M.A. Vorontsov, M.E. Kirakosyan and A.V. Larichev, Sov. J. Quantum Electron. 21 (1991) 105.
[6] G.B. Parrent and B.J. Thompson, eds., The new physical optics notebook, SPIE, Bellingham (1989).
[7] L.M. Soroko, Holography and coherent optics (Plenum Press, New York, 1980).
[8] Yu.D. Dumarevsky, N.F. Kovtonyuk and A.I. Savin, Image transformation in semiconductor-dielectric structures (Nauka, Moscow, 1987).
[9] S.A. Akhmanov, M.A. Vorontsov, V.Yu. Ivanov, A.V. Larichev and N.I. Zheleznikh, J. Opt. Soc. Am. B 9 (1992) 78.
[10] L.A. Vasiliev, Shade methods (Nauka, Moscow, 1968).
[11] M.A. Vorontsov and W.J. Firth, Phys. Rev. A 49 (1994) 2891.
[12] M.A. Vorontsov and I.P. Nikolaev, Proc. SPIE 2222 (1994) 413.
[13] S. Lowenthal and Y. Belvaux, Appl. Phys. Lett. 11 (1967) 49.